Received: 21 July 2020 | Accepted: 29 October 2020
DOI: 10.1002/hyp.13962

RESEARCH ARTICLE

WILEY

Characterizing spatial and temporal variation in ^{18}O and ^{2}H content of New Zealand river water for better understanding of hydrologic processes

Jing Yang | Bruce D. Dudley | Kelsey Montgomery | Will Hodgetts

National Institute of Water and Atmospheric Research, Christchurch, New Zealand

Correspondence
Jing Yang, National Institute of Water and Atmospheric Research, Christchurch 8011, New Zealand.
Email: jing.yang@niwa.co.nz

Funding information
New Zealand's Ministry for Business, Innovation and Employment

Abstract

Time series of hydrogen and oxygen stable isotope ratios (δ^2H and $\delta^{18}O$) in rivers can be used to quantify groundwater contributions to streamflow, and timescales of catchment storage. However, these isotope hydrology techniques rely on distinct spatial or temporal patterns of δ^2H and $\delta^{18}O$ within the hydrologic cycle. In New Zealand, lack of understanding of spatial and temporal patterns of δ^2H and $\delta^{18}O$ of river water hinders development of regional and national-scale hydrological models. We measured δ^2H and $\delta^{18}O$ monthly, together with river flow rates at 58 locations across New Zealand over a two-year period. Results show: (a) general patterns of decreasing δ^2H and $\delta^{18}O$ with increasing latitude were altered by New Zealand's major mountain ranges; δ^2H and $\delta^{18}O$ were distinctly lower in rivers fed from higher elevation catchments, and in eastern rain-shadow areas of both islands; (b) river water δ^2H and $\delta^{18}O$ values were partly controlled by local catchment characteristics (catchment slope, PET, catchment elevation, and upstream lake area) that influence evaporation processes; (c) regional differences in evaporation caused the slope of the river water line (i.e., the relationship between δ^2H and $\delta^{18}O$ in river water) for the (warmer) North Island to be lower than that of the (cooler, mountain-dominated) South Island; (d) δ^2H seasonal offsets (i.e., the difference between seasonal peak and mean values) for individual sites ranged from 0.50‰ to 5.07‰. Peak values of $\delta^{18}O$ and δ^2H were in late summer, but values peaked 1 month later at the South Island sites, likely due to greater snow-melt contributions to streamflow. Strong spatial differences in river water δ^2H and $\delta^{18}O$ caused by orographic rainfall effects and evaporation may inform studies of water mixing across landscapes. Generally distinct seasonal isotope cycles, despite the large catchment sizes of rivers studied, are encouraging for transit time analysis applications.

KEYWORDS

hydrologic processes, meteoric water line, river water, spatial and temporal distribution, stable isotope

1 | INTRODUCTION

Measurements of stable water isotopes have provided tools for a wide range of studies in hydrology, such as determining sources of flow and pathways of water across landscapes, quantifying surface—atmosphere water fluxes and surface–groundwater interactions, and transit time analysis (Cable, Ogle, & Williams, 2011; Kirchner & Allen, 2020; Lutz et al., 2018; Négrel, Petelet-Giraud, Barbier, & Gautier, 2003; Sprenger, Tetzlaff, Tunaley, Dick, & Soulsby, 2017). Surface water stable isotopes also provide useful tools in ecology, climate science, and food science (Gao & Beamish, 1999; Kelly, Heaton, & Hoogewerff, 2005). For example, $\delta^{18}O$ values can be used to infer natal origins of anadromous fish (Starrs, Ebner, & Fulton, 2016), and reconstruct palaeohydrology and paleoclimate records using the remains of biota that lived in surface water (Edwards, Wolfe, Gibson, & Hammarlund, 2004).

The major difference between traditional hydrology and isotope hydrology is that traditional hydrology takes all water molecule types as one single type (i.e., H_2O) when studying hydrologic processes, without distinguishing them into "light" water ($^1H_2{}^{16}O$) and "heavy" water ($^1H_2{}^{18}O$ and $^2H_2{}^{16}O$), while isotope hydrology utilizes the different thermodynamic characteristics of "light" and "heavy" water molecules which affect evaporation and condensation processes. This approach can provide a more precise description and quantification of different hydrologic processes. For example, precipitation that condenses at cooler temperatures tends to be more depleted in the heavier stable isotopes (Dansgaard, 1954, 1964); thus, precipitation falling at higher latitudes, at higher elevations, and further inland tends to be isotopically depleted (Craig, 1961a), allowing water from these areas to be traced as it subsequently moves across landscapes. Understanding of the processes governing the isotope values of precipitation has been greatly advanced by regional and global collection networks of precipitation data (Araguas-Araguas & Diaz Teijeiro, 2005; Baisden, Keller, Van Hale, Frew, & Wassenaar, 2016; Darling, Bath, & Talbot, 2003; IAEA/WMO, 2006; Katsuyama, Yoshioka, & Konohira, 2015; Kortelainen & Karhu, 2004; Schotterer, Oldfield, & Fröhlich, 1996), leading to the development of global and regional scale models of precipitation isotopes (Baisden et al., 2016; Bowen, 2010; Wassenaar, Van Wilgenburg, Larson, & Hobson, 2009).

Patterns in surface water isotope values are strongly dependent on spatial patterns of stable isotope values of precipitation within their catchments (Kendall & Coplen, 2001). However, isotope values of surface water differ from those of local precipitation due to processes that occur as water flows across landscapes, including mixing, sub-surface flows and evaporation (Gonfiantini, Fröhlich, Araguás-Araguás, & Rozanski, 1998; McDonnell, Stewart, & Owens, 1991; Sprenger et al., 2017). These processes can be modified by anthropogenic activity (e.g., dam construction and water abstraction for irrigation and industry) which redistribute water spatially and temporally and can intensify evaporation processes. Statistical approaches to calculate mixing (e.g., of surface waters and groundwater) can benefit from understanding of spatial patterns of surface water isotopes, in addition to groundwater and rainfall isotopes (e.g., Kuhlemann & Soulsby, 2020). For example, in New Zealand, understanding of surface water/groundwater interactions currently relies heavily on hydrologic modelling (e.g., Yang, McMillan, & Zammit, 2017) which depends on model calibration of streamflow records. Improved understanding of areas nationally where surface waters and groundwaters are isotopically distinct would aid current efforts to improve calibration of these models; source partitioning using stable isotope tracers tends to be more reliable where water sources of interest are sufficiently isotopically distinct, relative to the degree of statistical noise in the system.

Analytical methods to calculate timescales of storage in catchments benefit from understanding of seasonal cycles of stable isotopes in river water as well as precipitation. For example, "young water fraction" (F_{yw}) calculations (Jasechko, Kirchner, Welker, & McDonnell, 2016; Kirchner, 2016; von Freyberg, Allen, Seeger, Weiler, & Kirchner, 2018) rely on sufficient seasonal fluctuations of isotope values of precipitation and river water (i.e., $\delta^{18}O$ and δ^2H seasonal offsets). The degree of damping of the precipitation seasonal cycle seen in river water can then be used to calculate timescales of storage in catchments. Seasonal precipitation isotope cycles in New Zealand tend to show relatively small amplitudes (for a country of New Zealand's latitude) due to the predominant oceanic climate (Allen et al., 2019; Feng, Faiia, & Posmentier, 2009). Furthermore, precipitation stable isotope values in New Zealand are strongly influenced by differences in the origins of moisture sources to the country, which may add non-cyclical variation to precipitation isotope time series (Baisden et al., 2016). However, some areas of New Zealand may be more appropriate than others for estimation of F_{yw} based on stable isotope measurements. For example, some inland regions of the country show relatively large seasonal variations in temperature; it is likely that there are regional differences in "temperature effects" on stable isotope values of precipitation across New Zealand, and thus seasonal amplitudes of stable isotope values of precipitation. For some sites on large rivers, F_{yw} is likely to be low; damping of seasonal tracer cycles is higher when catchment residence times are great. In these catchments the goodness of fit of the model for estimation of F_{yw} tends to decrease (Soulsby & Tetzlaff, 2008), leading to reduced certainty in F_{yw} estimates (Lutz et al., 2018). Therefore, long-term, nationally representative sampling of river water isotope values across a range of catchment sizes is necessary to provide broad-scale data for the development of transit time models, and mixing studies.

Currently, maps of surface water isotope values for New Zealand exist for deuterium only, and are based on a combination of long-term regular sampling of selected rivers, alongside one-off sampling with higher spatial resolution (Stewart, Cox, James, & Lyon, 1983; Stewart & Taylor, 1981). Although studies on young water fraction have been conducted in an inland catchment of New Zealand's South Island (Marttila, Dudley, Graham, & Srinivasan, 2017), there is a need to apply this approach nationally. In this study, our objectives were: (a) to describe spatial patterns of river water $\delta^{18}O$ and δ^2H values, and deuterium excess (d-excess) across New Zealand to inform future research into mixing between surface and groundwaters; (b) examine the environmental factors that affect these spatial distributions; and (c) to describe seasonal offsets of $\delta^{18}O$ and δ^2H in river waters, to facilitate future calculations of water age distributions and young

water fractions. These developments will provide a better understanding of hydrologic processes in New Zealand, and improve integrated surface- and groundwater management.

2 | METHODS

2.1 | Water sampling network

River water samples were collected from sites on NIWA's existing New Zealand River Water Quality Network (NZRWQN; Smith & Maasdam, 1994). These 58 sites (Figure 1 and Table 1) span 35 of New Zealand's major river systems, and 49 rivers in total. Sites in the NZRWQN were selected over a wide range of locations, elevations, catchment sizes and geomorphological environments to be representative of the spatial states and trends of all New Zealand's rivers (Davies-Colley et al., 2011). The rivers which are sampled drain approximately 50% of the land area of the South Island and 40% of the North Island, with catchment areas ranging from 19 to 20,582 km^2 and maximum catchment elevations ranging from 107 to 1,422 m.

2.2 | Sample collection and analysis

Samples were taken on a monthly basis over two continuous years (April 2017 to March 2019), and river flow rates were recorded at the time when samples were collected. Variation resulting from diurnal patterns was minimized by collection of samples at similar times of the day. All samples were subjected to similar conditions upon collection; each was stored in 100 ml tube in an insulated ice bin, keeping samples at approximately 0°C and in darkness in the field, and then frozen and stored at approximately −20°C in the laboratory and later thawed for analyses (Davies-Colley et al., 2011). This methodology was employed to reduce alteration of isotope values due to evaporation after sampling, and consistency of these methods across sites was maintained to removes variability in evaporation (e.g., between summer and winter or between northern and southern sites).

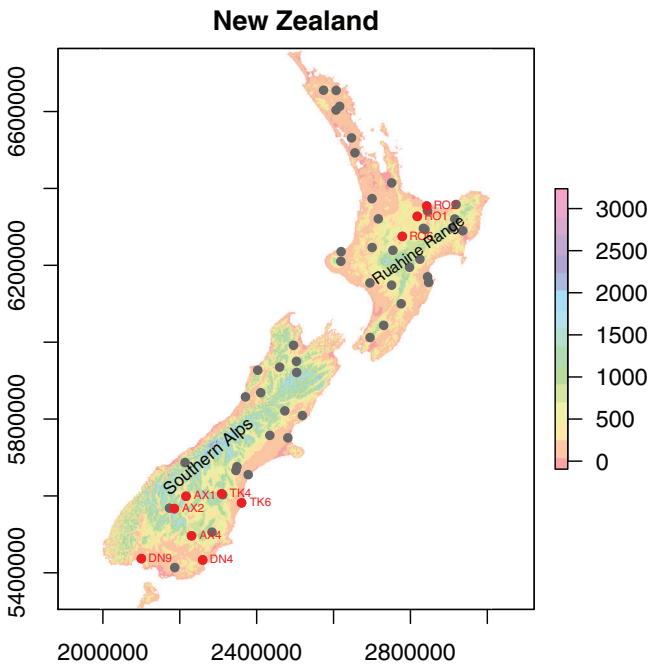

FIGURE 1 Topography, and river water isotope sampling sites (dots) across New Zealand. Red dots and site labels indicate >5% upstream catchment area is covered by wetland, lakes and reservoirs (termed "lake(s)" collectively)

In the lab, each sample was thawed while sealed, then gently agitated and sub-sampled into a 2 ml vial and labelled with its unique identifier along with the date of collection. Isotope analyses were conducted at the National Institute of Water and Atmospheric Research (NIWA) in Christchurch, New Zealand. The δ^2H and $\delta^{18}O$ values for water samples were measured by isotope ratio infrared spectroscopy (IRIS) on a wavelength-scanned, cavity ring-down spectrometer (WS-CRDS) model L1102-i (Picarro, Sunnyvale, CA). Samples were analysed against three internal laboratory reference materials calibrated to Vienna Standard Mean Ocean Water (VSMOW) to avoid contamination from previous samples, and the spectrometer was set to analyse each sample eight times with only the final three for each vial being used. Standard deviations were less than 0.1‰ for $\delta^{18}O$ and less than 1‰ for δ^2H. We used Picarro Chem Correct post-processing software to derive final $\delta^{18}O$ and δ^2H values. Standards were cross-checked at two external laboratories: GNS Science Stable Isotope Laboratory (WS-CRDS isotopic water analyser model IWA-45EP, Los Gatos Research, Mountain View, CA) and NIWA Wellington Stable Isotope Analytical Facility (model Delta V IRMS, Thermo Scientific, Waltham, MA). A subset of 20 δ^2H and $\delta^{18}O$ samples from the final dataset was also cross-checked at the GNS Science Stable Isotope Laboratory.

2.3 | Data analysis

Meteoric water lines (i.e., the relationship between δ^2H and $\delta^{18}O$ in precipitation and water bodies derived from precipitation) can be used to study evaporation and mixing processes of surface waters (Gammons et al., 2006; Putman, Fiorella, Bowen, & Cai, 2019). Following (Landwehr & Coplen, 2006), we reserve the term "meteoric water line" (MWL) to describe the linear relationship between $\delta^{18}O$ and δ^2H in precipitation and use the term "river water line" (RWL) for the linear relationship between $\delta^{18}O$ and δ^2H in river waters. The Global Meteoric Water Line (GMWL) giving the relationship between $\delta^{18}O$ and δ^2H for global average precipitation values (Craig, 1961a), will be used as a reference. Since periods of high flow tend to be isotopically similar to recent precipitation (von Freyberg et al., 2018), we compared flow-weighted and unweighted river water lines. Furthermore, we also calculated Local River Water Lines (LRWL) representing local precipitation and evaporation processes, which are influenced by local climate, geology, and land-cover (Isokangas et al., 2017) for each sampling site. Where multiple sites were located within the same connected river network, we compared LRWLs for upstream and downstream sites.

TABLE 1 Stable isotope sampling site information for all NZRWQN sites

Site code	Elevation (m)	Latitude (°)	Longitude (°)	Site code	Elevation (m)	Latitude (°)	Longitude (°)
AK1	15	−36.38	174.51	NN1	76	−41.26	172.82
AK2	10	−36.73	174.62	NN2	376	−41.63	172.91
AX1	305	−44.73	169.28	NN3	655	−41.89	172.92
AX2	305	−45.01	168.88	NN5	183	−41.76	172.39
AX3	320	−44.99	168.72	RO1	320	−38.18	176.51
AX4	91	−45.66	169.41	RO2	6	−37.93	176.77
CH1	442	−42.79	172.54	RO3	185	−38.46	176.70
CH2	60	−42.90	173.10	RO4	205	−38.48	176.75
CH3	244	−43.36	172.06	RO5	3	−38.04	176.80
CH4	76	−43.42	172.63	RO6	349	−38.66	176.08
DN2	220	−45.60	170.09	TK1	4	−44.27	171.34
DN4	9	−46.24	169.75	TK2	180	−44.17	170.94
DN5	15	−46.39	168.79	TK3	238	−44.08	170.98
DN9	14	−46.13	167.68	TK4	250	−44.70	170.45
GS1	55	−38.47	177.88	TK5	198	−44.73	170.49
GS2	457	−38.42	177.56	TK6	5	−44.93	171.10
GS3	425	−38.20	177.62	TU1	131	−38.94	175.19
GS4	11	−37.86	177.64	TU2	363	−39.00	175.81
GY1	15	−41.83	171.70	WA1	15	−39.05	174.26
GY2	20	−42.45	171.30	WA2	320	−39.28	174.25
GY3	171	−42.36	171.78	WA4	18	−39.77	175.15
GY4	53	−43.94	169.30	WA5	518	−39.81	175.81
HM1	80	−38.27	175.35	WA7	152	−40.24	176.12
HM2	10	−37.80	175.15	WH1	30	−35.28	173.69
HM6	10	−37.42	175.72	WH2	10	−35.28	174.05
HV2	26	−39.71	176.93	WH3	21	−35.74	174.05
HV3	2	−39.59	176.89	WH4	91	−35.65	174.15
HV4	488	−39.38	176.33	WN2	200	−41.05	175.19
HV6	320	−39.18	176.63	WN5	268	−40.76	175.60

We used deuterium excess (d-excess), defined as d-excess = $\delta^2H - 8\,\delta^{18}O$ (Dansgaard, 1964), to quantify the deviation away from the GMWL, which can be used as an index of post-precipitation evaporation in water. Kinetic fractionation occurs most strongly during rapid evaporation, and causes a deviation of water line from the meteoric water line due to the mass difference between water molecules containing deuterium ($H^1D^2O^{16}$ = 19 g/mol) and heavy oxygen ($H^1H^1O^{18}$ = 20 g/mol) causing more fractionation of heavy oxygen. Evaporation effects on the $\delta^{18}O$ to δ^2H relationship in water bodies are strongest where the reservoir of surface water is small, replacement of water is low, humidity is low, and the evaporation rate is high; for example, shallow water bodies with long residence times in warm, windy climates are likely to show very negative values of d-excess. We generated national maps of δ^2H, $\delta^{18}O$ and d-excess using the R software package (R Core Team, 2018). Interpolations between sites were made using the inverse distance weighted method (IDW).

We examined relationships between river water isotopes and environmental factors by comparing mean $\delta^{18}O$ and δ^2H values for each site to environmental variables with correlation analysis. These environmental factors include latitude, upstream lake area, catchment elevation, PET and catchment slope. We examined the effects of upstream lakes, reservoirs and wetlands, hereinafter termed "lakes" collectively. Environmental variables were taken from the River Environmental Classification (REC; Snelder, Biggs, & Woods, 2005) and FENZ (Leathwick et al., 2010) geodatabases. These databases provide environmental data on the upstream catchments for each reach in the New Zealand river network.

We analysed seasonal periodicity of river water $\delta^{18}O$ by fitting a sinusoidal function to monthly averaged isotope $\delta^{18}O$:

$$\hat{\delta}^{18}O = A\sin(2\pi t + \varphi),$$

where A is amplitude, t is the time lag in years and φ is the phase. The difference of this seasonal periodicity was also examined between sites in South Island and North Island.

We generated maps of long-term average $\delta^{18}O$ and $\delta^{2}H$ and d-excess in precipitation using the regression equations of Baisden et al. (2016) applied to monthly climate data from the NIWA virtual climate station network (VCSN; Tait, 2008) for the period 1997–2018.

3 | RESULTS

3.1 | The national river water line

Figure 2a,b shows the River Water Line for New Zealand (NRWL), and the Global Meteoric Water Line (GMWL) is listed as a reference. The NRWL (Figure 2a) was obtained through a linear regression analysis of all 1,359 samples with the form $\delta^{2}H = 8.44\ \delta^{18}O + 14.83$ ($r^2 = 0.98$), compared to GMWL $\delta^{2}H = 8.17\ \delta^{18}O + 10.35$ from Craig (1961b). Both the slope and intercept of the NRWL (i.e., 8.44 and 14.83, respectively) are larger than those of the GMWL (i.e., 8.17 and 10.35), the National Meteoric Water Line based on samples of precipitation collected around New Zealand (∼7.86 and 10.34; Baisden et al., 2016), and a one-off sampling campaign of small drainage basins in the South Island of New Zealand (8.16 and 10.54; Lachniet, Moy, Riesselman, & Stephen, 2018). This may in part be due to spatial patterns of local hydrological processes. For example, evaporation is relatively high at sites towards the south of the South Island where upstream lake area is high (Figures 1 and 2c), and mean annual evaporative ratio—based on estimated average annual evaporation and rainfall for 1960 ∼ 2006 in New Zealand by Tait, Henderson, Turner, and Zheng (2006) and Tait et al. (2006)—is high (Figure 5d). These effects are discussed in more detail below. Figure 2b shows the site averaged water lines with flow weighted average (NRWLF) and simple arithmetic average (NRWLA). However, these two fitted water lines are very similar, indicating that the effect of streamflow is generally minimal. These two lines are not very different from the NRWL (Figure 2a), and the small difference is mainly attributed from seasonal variations in precipitation isotope values.

Figure 2c shows a substantial difference between the river water lines in the North Island (RWLN) and South Island (RWLS), with regressed lines $\delta^{2}H = 6.99\ \delta^{18}O + 6.8$ ($r^2 = 0.94$), and $\delta^{2}H = 9.27\ \delta^{18}O + 21.56$ ($r^2 = 0.97$), respectively. The majority of isotope values ($\delta^{2}H$ and $\delta^{18}O$) are higher in the North Island than in the South Island, that is, $\delta^{18}O$ ranged from −8.7 to −2.6‰ in North Island and −11.7 to

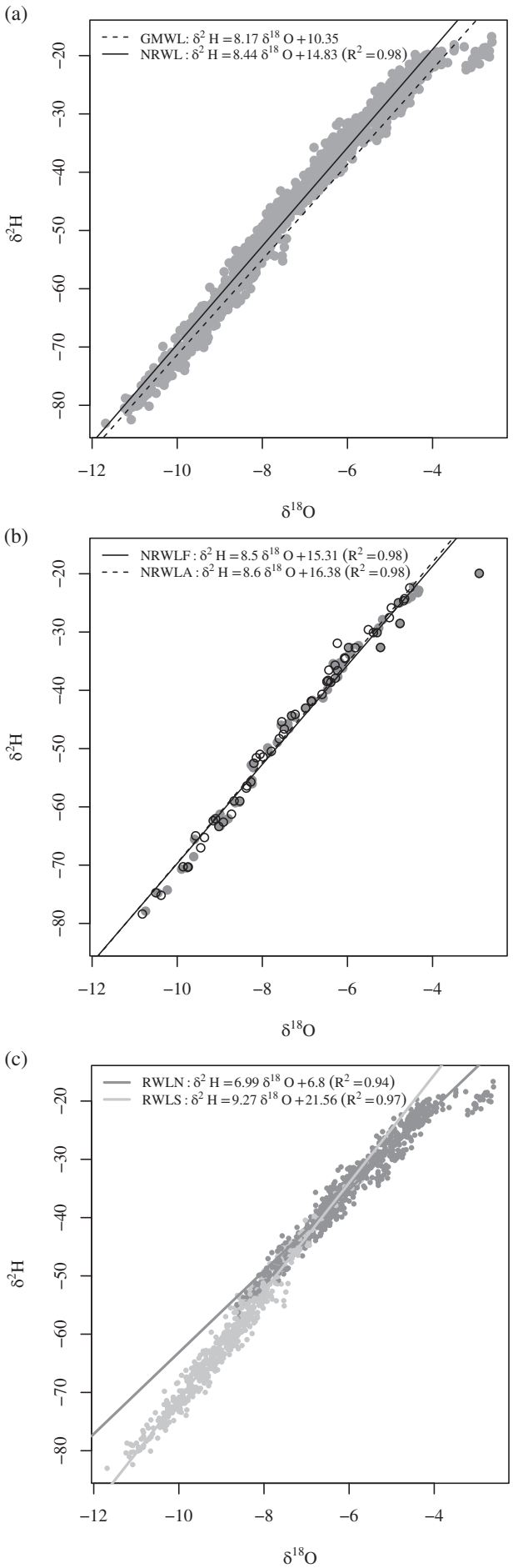

FIGURE 2 Relations between $\delta^{18}O$ and $\delta^{2}H$ for (a) the entire national dataset, (b) the arithmetic (dashed) and flow weighted (solid) means over sites, and (c) North Island (black) and South Island (grey) datasets. GMWL, Global Meteoric Water Line; NRWL, National River Water Line; NRWLA, National River Water Line using arithmetic site means; NRWLF, National River Water Line using flow-weighted site means; RWLN, River Water Line for North Island sites; RWLS, River Water Line for South Island sites

−5.7‰ in South Island, while δ^2H ranged from −57.2 to −16.6‰ in North Island and −82.9 to −33.5‰ in South Island.

3.2 | Local river water lines and d-excess

Figure 3 shows the local river water lines (LRWL) for each site and Table 2 lists the corresponding slopes and intercepts for each linear regression. Compared to the NRWL, the ranges of sampled isotopes for each site are very narrow, and regression slopes range from 4.3 to 8.85 while intercepts range from −7.95 to 16.1. Site d-excess means ranged from 3.49 to 15.49 (Table 2).

Coloured lines in Figure 3 represent LRWLs influenced by lakes—categorized as those for which lakes cover more than 5% of the total upstream catchment area. The impact of lakes on d-excess is illustrated by the relationship in the bottom left panel of Figure 3, which

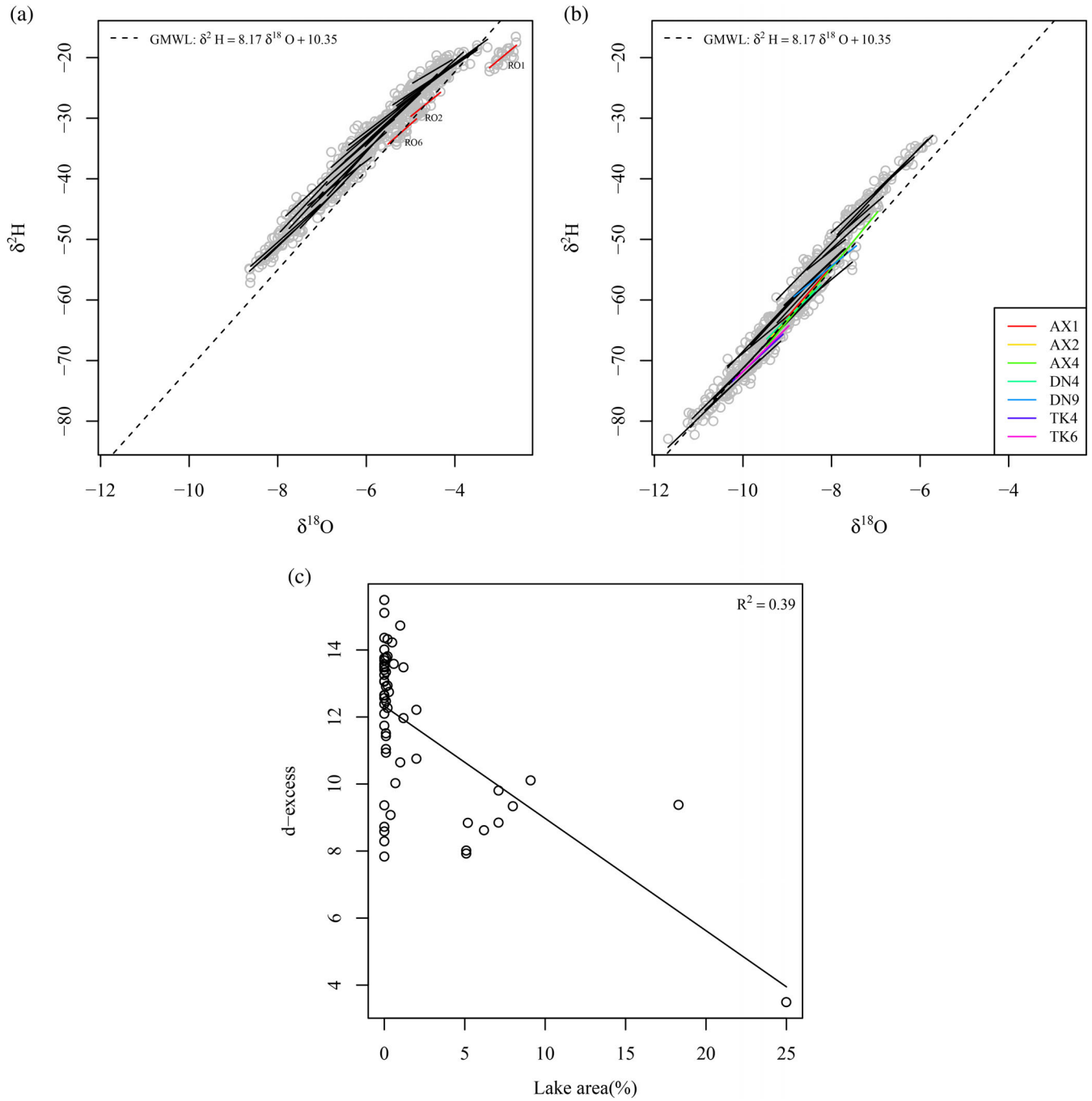

FIGURE 3 LMWLs of 58 river sites across New Zealand split across (a) the North Island and (b) the South Island. Colour lines mark the sites below lakes as shown in Figure 1. Panel (c) shows the relationship between d-excess and upstream lake area (as a percentage of upstream catchment area) for all sites

TABLE 2 Time-averaged d-excess, and slopes and intercepts of local river water lines for all NZRWQN sites

Site	d-excess	Slope	Intercept	Site	d-excess	Slope	Intercept
AK1	12.57	4.95	−1.46	NN1	12.64	6.32	0.27
AK2	11.74	5.40	0.41	NN2	12.66	5.77	−5.65
AX1	9.34	8.46	13.25	NN3	11.43	7.80	9.55
AX2	8.85	8.08	9.55	NN5	12.22	6.70	2.05
AX3	9.07	7.25	1.21	RO1	3.49	6.07	−2.11
AX4	8.62	8.85	16.15	RO2	9.81	5.88	−0.31
CH1	10.76	6.85	1.29	RO3	13.07	7.25	7.83
CH2	10.65	6.87	1.32	RO4	13.52	6.41	3.21
CH3	11.05	7.99	10.99	RO5	12.74	7.45	9.24
CH4	10.94	7.77	8.84	RO6	9.38	6.47	1.38
DN2	9.37	6.08	−7.95	TK1	8.72	7.80	6.70
DN4	8.84	7.29	2.51	TK2	8.59	7.54	4.21
DN5	10.03	7.92	9.31	TK3	8.29	7.02	−2.21
DN9	10.11	5.94	−6.89	TK4	7.92	6.78	−3.95
GS1	12.39	8.23	13.85	TK5	7.83	6.67	−5.83
GS2	13.07	6.96	6.00	TK6	8.02	7.31	1.24
GS3	12.94	6.47	3.57	TU1	14.32	6.44	4.53
GS4	14.01	6.61	5.75	TU2	14.72	7.84	13.50
GY1	13.58	7.69	11.32	WA1	13.76	5.53	0.98
GY2	13.48	7.17	8.12	WA2	15.49	6.32	4.81
GY3	14.23	6.68	4.57	WA4	13.78	6.13	2.70
GY4	13.48	7.52	9.50	WA5	13.35	6.48	1.37
HM1	13.81	6.75	6.63	WA7	12.1	5.54	−3.83
HM2	12.91	6.99	7.51	WH1	13.58	4.31	−2.84
HM6	13.05	7.36	9.67	WH2	11.97	5.33	0.42
HV2	11.51	7.70	9.52	WH3	13.41	4.78	−1.97
HV3	12.47	6.99	4.74	WH4	12.27	6.73	6.55
HV4	13.26	6.65	2.22	WN2	15.11	5.82	2.15
HV6	13.69	7.86	12.66	WN5	14.36	6.75	6.62

shows declining d-excess as lake area increases (R^2 0.37; ANOVA $p < 10^{-7}$), indicating that d-excess tends to decrease as a result of upstream evaporation from surface water.

Figure 4 demonstrates the effects of different hydrologic processes along the river networks of two regions (one in the North Island and the other in the South Island). In the North Island example, the region consists two neighbouring basins: the Tarawera basin and the Rangitaiki basin. In the Tarawera basin, river water from Lake Tarawera (RO1) becomes isotopically depleted by mixing downstream waters that have not undergone such significant evaporation to give the composition at site RO2; while in the Rangitaiki basin, there is an increasing input of lower elevation rainfall with higher δ values along the river, with no evidence of enrichment by evaporation. In the South Island example, sites AX1 and AX2 are enriched (lake-influenced), AX3 is the most depleted reflecting the small tributary source, and sites AX4 and DN4 represents a mixing of the waters from upstream rivers and tributaries.

3.3 | Spatial distribution of isotopes in river water

Figure 5 shows spatially interpolated δ^2H and $\delta^{18}O$ and d-excess values, based on the inverse-distance weighted method. Nationally, time-averaged site means for $\delta^{18}O$ of river waters ranged from −11.7 to −2.6‰, δ^2H from −82.9 to −16.6‰, and d-excess from 3.49 to 15.49 (Table 2). However, as shown in Figure 2, these ranges differed between the South Island and North Island. These differences in stable isotope distributions correspond to differences in latitude and are also likely due to increases in catchment elevation in South Island sites, where the Southern Alps mountain range strongly affects regional climate and hydrology; Baisden et al. (2016) found elevation to be highly significant predictor of precipitation isotope values in New Zealand. The "latitude effect" (Gibson, Birks, & Edwards, 2008) is a result of increasing rainout and decreasing evaporation with increased latitude.

There is an evidence in Figure 5 that δ^2H and $\delta^{18}O$ values decrease from West to East (especially in Hawkes Bay on the east

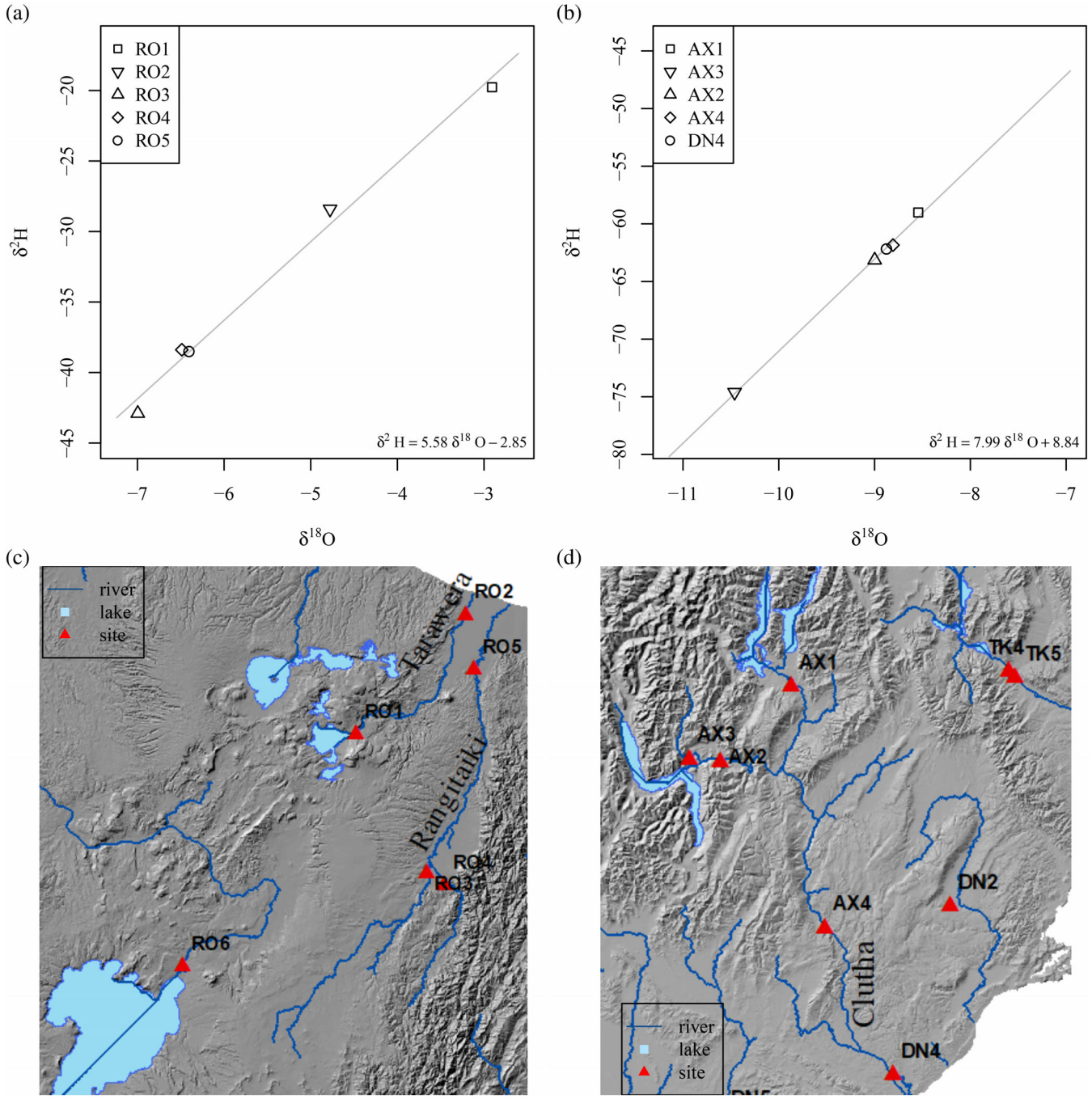

FIGURE 4 Relations between mean $\delta^{18}O$ and mean $\delta^{2}H$ of river waters for (a) two neighbouring North Island basins (Tarawera basin and Rangitaiki basin) and (b) for Clutha basin in the South Island in South Island. Panels (c) and (d) show maps of the Tarawera and Rangitaiki basins, and Clutha basin, respectively

coast of the North Island and Canterbury plains on the east coast of the South Island). This highlights variance from West to East in elevations, as well as New Zealand's prevailing West-Southwesterly winds, and dominant western moisture source, which also causes rainfall to reduce from West to East (Salinger & Mullan, 1999). This pattern is especially obvious in the South Island where the Southern Alps extend most of the length of the island. The highest d-excess values were found in the rivers of central New Zealand (i.e., south of the North Island and north of the South Island), with peak values in Southwest of the North Island. Lowest d-excess values were apparent in rivers in rain-shadow areas to the east of the central ranges of the North Island, and the Southern Alps of the South Island.

3.4 | Relationships with environmental factors

Figure 6 shows relationships of $\delta^{2}H$ with catchment environmental factors. All four of the factors in these plots influence the evaporation processes of water (and $\delta^{2}H$ values of precipitation in the case of latitude and catchment elevation) and thus water isotopes in

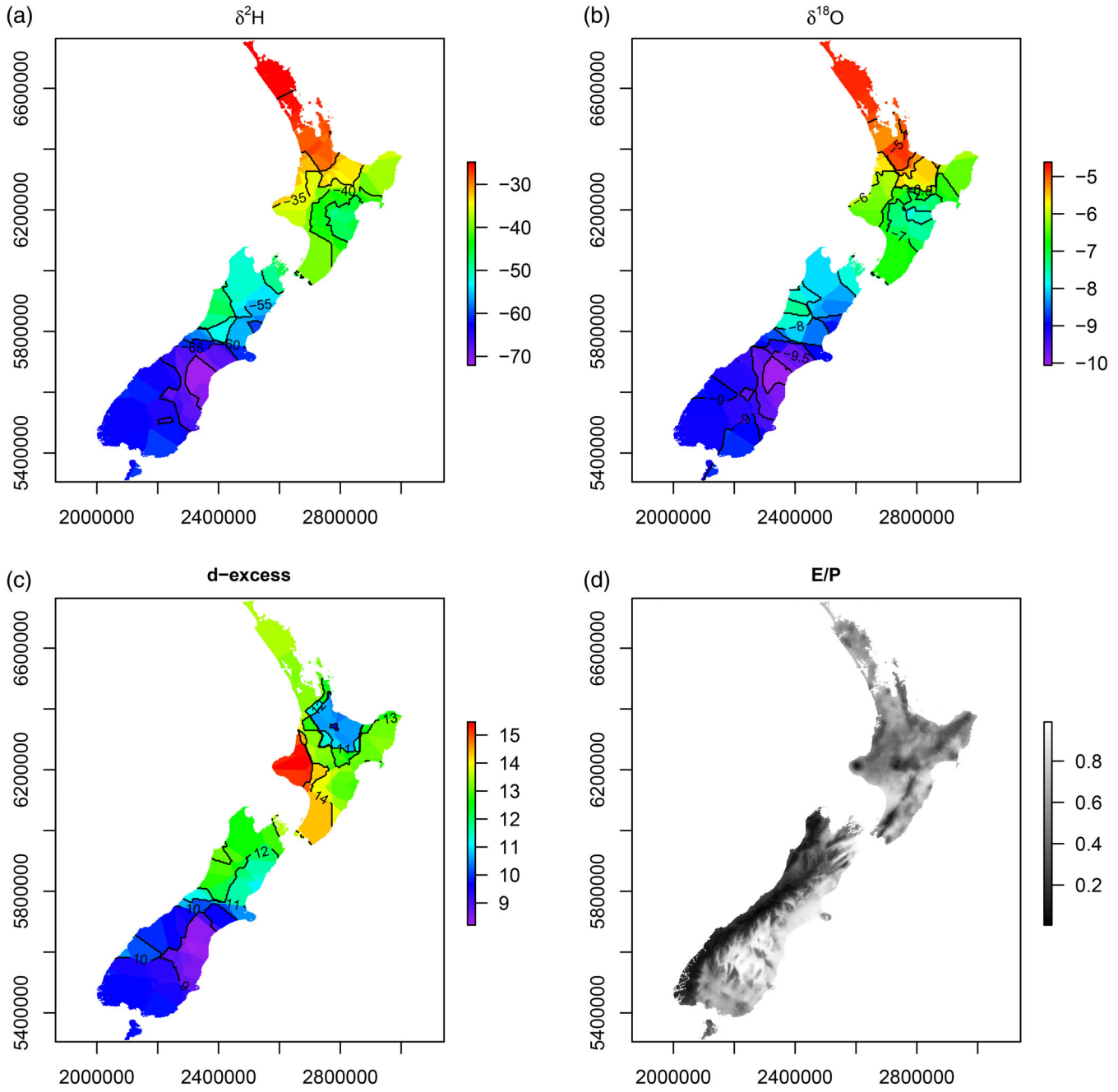

FIGURE 5 Spatial distribution of mean δ^2H (a), $\delta^{18}O$ (b) and d-excess (c) of river waters in New Zealand, interpolated with the inverse-distance weighted (IDW) method. Panel (d) shows mean annual evaporative ratio. E/P, evaporation over precipitation

downstream rivers. Since there is a relationship between δ^2H and $\delta^{18}O$ (as discussed above), similar results should be expected for $\delta^{18}O$. δ^2H has a positive correlation with latitude (R = 0.88) and PET (R = 0.67) but negative correlations with catchment slope (R = –0.42), and catchment elevation (R = –0.72).

3.5 | Seasonal variations

Isotopic samples were grouped into North Island and South Island datasets. Seasonal variations of δ^2H, obtained by subtracting monthly values from site means, are shown in Figure 7, for the North and South Islands, respectively. The black curves give the sine curve fit for these variations, revealing periodic cycles. Our results revealed differences between the North Island and South Island in timing of seasonal peaks, which may reflect differences in storage; in the North Island, δ^2H reaches its maximum in February (late summer) and minimum in August (late winter), while in the South Island, it reaches its maximum in March and minimum in September. Across all sites, modelled δ^2H peak amplitudes ranged from 0.50‰ (Site WA7 on the Manawatu River, Central North Island, with a catchment area of 761 km^2) to 5.07‰ (Site DN2 on Sutton Stream, Central Otago, with a catchment area of 151 km^2).

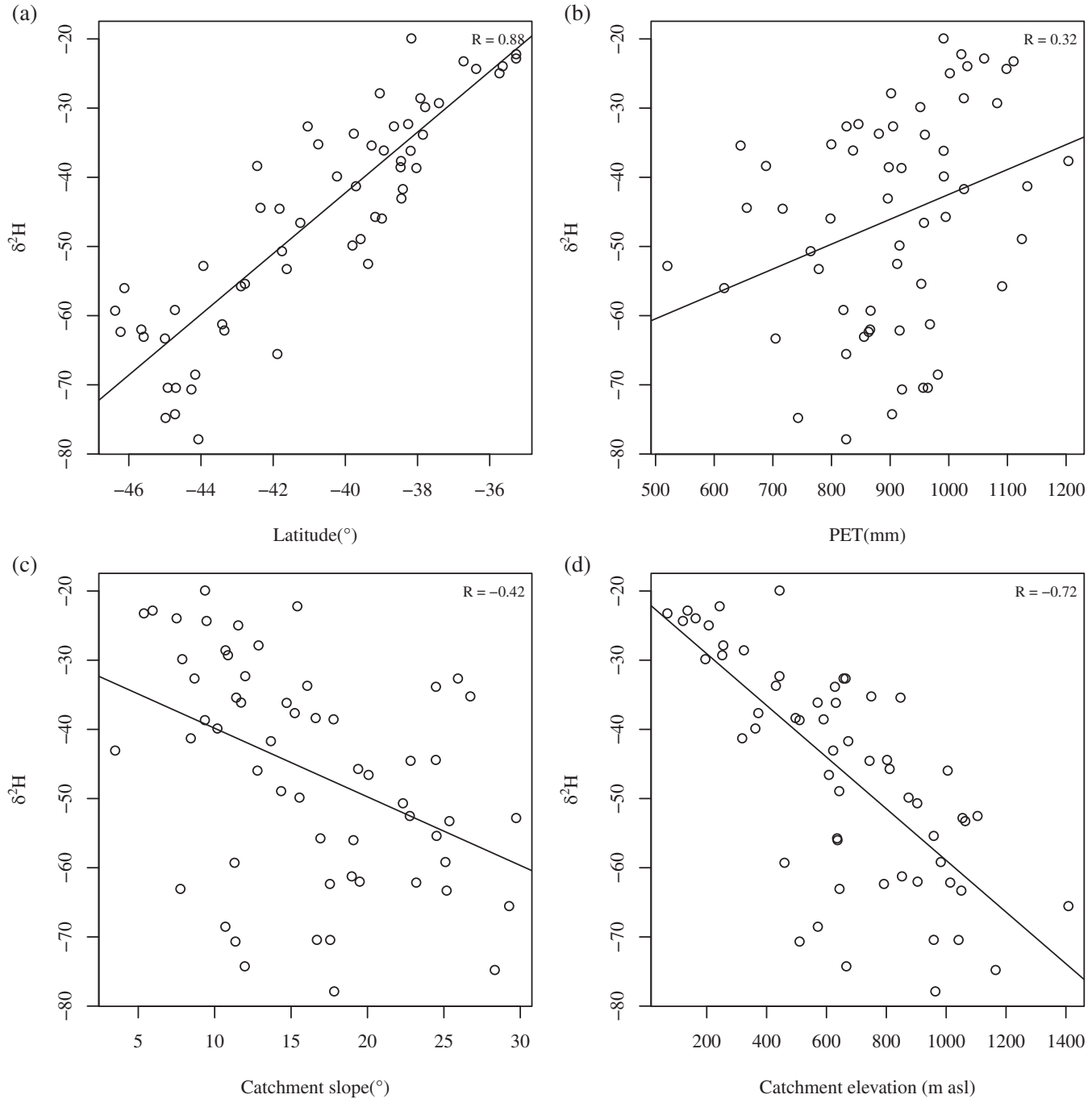

FIGURE 6 Relationships between catchment environmental factors and δ^2H of river water at all NZRWQN sites

4 | DISCUSSION

4.1 | Spatial patterns of river water $\delta^{18}O$ and δ^2H values

Our results show spatial patterns of $\delta^{18}O$ and δ^2H that reflect New Zealand's large latitude range, and strong orographic rainfall effects caused by its central mountain ranges. Lower δ^2H and $\delta^{18}O$ in rivers at higher latitudes reflect the impact of lower δ^2H and $\delta^{18}O$ in precipitation (Figure 8), following the temperature gradient between the equator and the poles (Dansgaard, 1964), but also may stem from enrichment during evaporation of lake and river water. The observed regional-scale patterns include low $\delta^{18}O$ and δ^2H values in river water derived from high-elevation precipitation across New Zealand. Clear differences between the $\delta^{18}O$ and δ^2H values of river water and precipitation at low elevations were seen particularly in dry, leeward areas of the country. These patterns are useful for studies that infer water sources and mixing in rivers (as shown in Figure 4), and for mixing between river and groundwaters. For example, major rivers with high-elevation catchments have been identified as the dominant

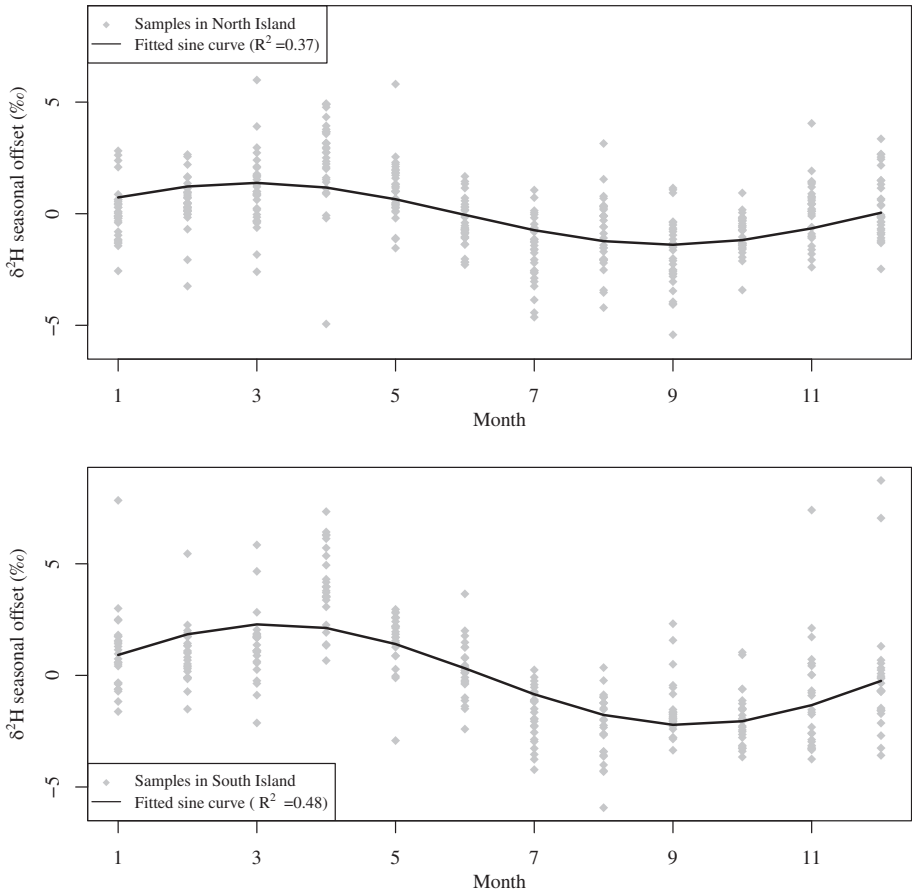

FIGURE 7 Seasonal variations of δ^2H in North Island, and South Island (grey), with corresponding fitted sine curves (dots: δ^2H anomaly samples; solid curves: fitted sine curves)

source of recharge to confined gravel aquifers in lowland Canterbury, due largely to differences in δ^{18}O values between river water and potential local water sources (Klaus & McDonnell, 2013; Taylor et al., 1989). Patterns of isotopically depleted river water, relative to lowland precipitation, are caused by New Zealand's prevailing west to south-west maritime winds crossing the country. As weather fronts reach the west coast and begin to rise, condensation and precipitation increase with elevation. The proportion of heavy isotopes lost to precipitation is greatest initially, where precipitation begins. This ratio progressively decreases with increasing elevation and rainout. δ^{18}O and δ^2H values progressively decrease within precipitation at higher elevation (Gonfiantini, Roche, Olivry, Fontes, & Zuppi, 2001) and therefore distance inland. This causes a depletion in west coast river waters with increasing catchment elevation. Isotopic depletion also occurs in rivers on the east of New Zealand, when fed by a westerly moisture source, especially those fed by high elevation catchments. For some rivers in the Canterbury plains (e.g., the Rangitata, Rakaia and Waimakariri Rivers), this depletion is likely to be enlarged still further by glacier-derived water and snowmelt from the Southern alps (e.g., Ala-Aho et al., 2018; Hales & Roering, 2009). The isotope contour lines of −8‰ for δ^{18}O and −50‰ for δ^2H (South Island in Figure 5) follow the ridgeline of the Southern Alps, highlighting these elevation effects (Gonfiantini et al., 2001). This spatial pattern is partly similar to patterns in Japan, where water vapour carried by maritime winds also encounters steep slopes upon reaching land (Katsuyama et al., 2015). Islands such as New Zealand, Japan, Hawaii, and the British Isles may be commonly affected by orographic effects on maritime winds, and to some extent and have similar spatial patterns of δ^{18}O and δ^2H values in precipitation and surface waters (Darling et al., 2003; Scholl, Ingebritsen, Janik, & Kauahikaua, 1996).

The geospatial approach used for this initial mapping (based on inverse-distance weighted method) does not incorporate environmental predictors of precipitation isotopes (e.g., elevation, latitude), or catchment scale modelling (Bowen, Kennedy, Liu, & Stalker, 2011; West, February, & Bowen, 2014). The relationships between spatial patterns of river water isotopes and environmental drivers (in Figures 3 and 6) suggest that modelling approaches incorporating these environmental drivers should result in improved river water isotope predictions at finer scale. It is worth noting that the relationships with environmental variables shown in Figure 6 do not distinguish between the effects of rainfall isotope values and hydrological processes in surface and groundwaters. It is possible however that the positive relationship between PET and river water δ^{18}O and δ^2H values is partly driven by evaporation from surface waters. In contrast, increasing catchment slope, which leads to faster water routing in the catchment, therefore gives less chance for water to evaporate. Similarly, a secondary effect of increasing catchment elevation and latitude (as well as isotopically depleted precipitation) is that lower temperature will potentially result in less evaporation, and less isotopic enrichment of surface water. Enrichment of isotope values of

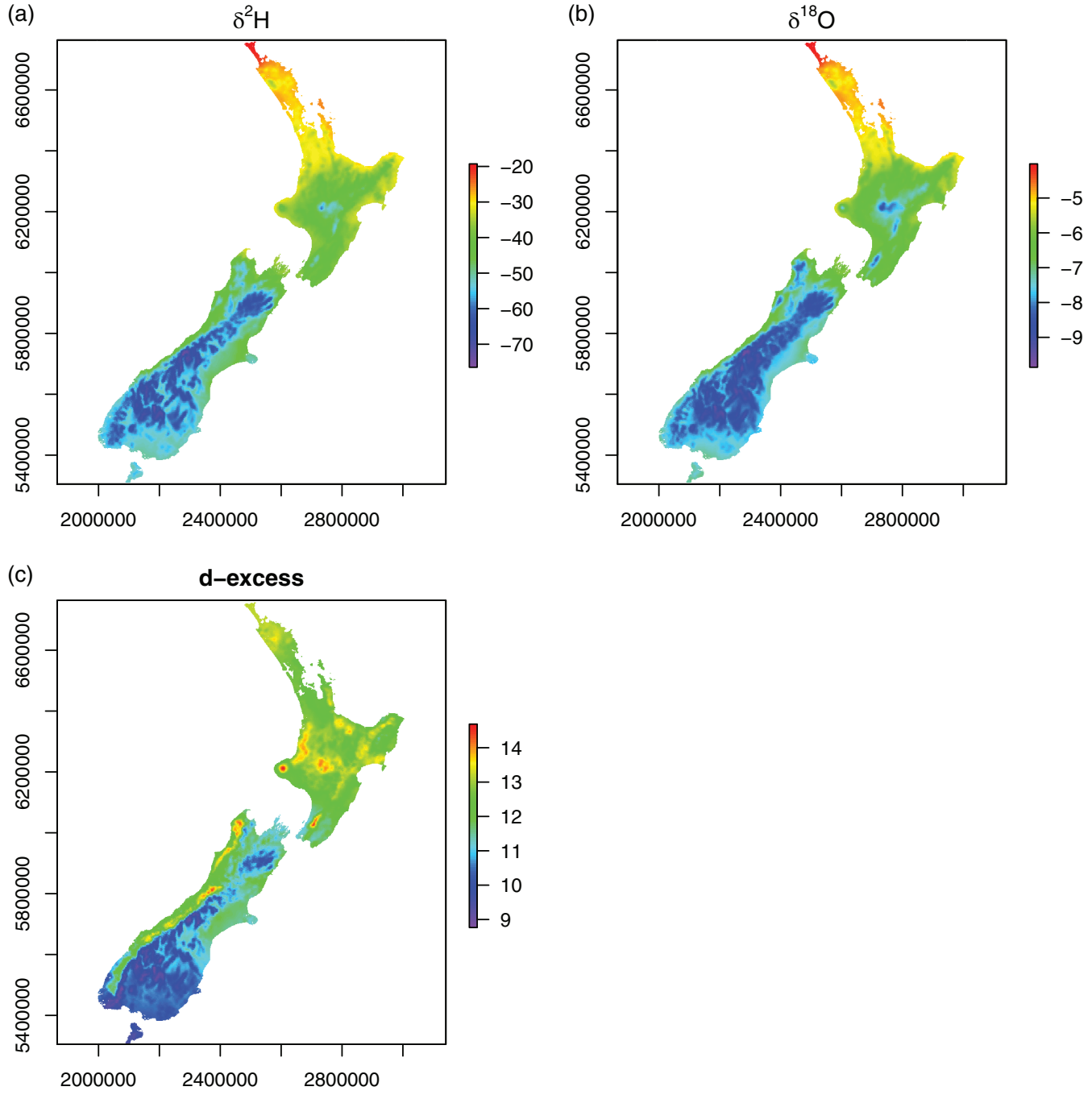

FIGURE 8 Spatial distribution of mean δ^2H (a) and δ^{18}O (b) and d-excess (c) of precipitation in New Zealand, averaged over the monthly predictions from 1997 to 2018 based on the regression models in Baisden et al. (2016)

water downstream by evaporation processes in lakes and wetlands can be seen particularly in Figures 2a and 3a, where sites downstream from lakes in the North Island plot are below the national river water line. Because catchments with large areas of wetlands and lakes upstream do not vary spatially in the same way as other drivers of surface water isotopes (such as climate and elevation), the inverse distance weighted method used for our mapping (Figure 4) may incorrectly extend these effects out over regions, particularly where sites are sparse.

The geographical position of lakes in the North Island, and other lakes and wetlands may contribute to differences between the relative slopes of the North and South Island river water lines. As seen in Figure 1, the majority of sites for which >5% of the upstream catchment area is covered by lakes are in the North East of the North Island, where precipitation δ^{18}O and δ^2H values are among the most enriched in the country, and in the south of the South Island, where precipitation δ^{18}O, δ^2H and d-excess values are most depleted (Baisden et al., 2016) and many of the large, alpine-fed rivers are

dammed for hydropower generation. Lakes along the river network not only increase the travel time of river water, but also increase the surface water area. Both these factors cause increases in evaporation, especially in lowland areas, and therefore departure from the NRWL. Those sites below lakes include RO1 and RO2 below Lake Tarawera, RO6 below Lake Rotoroa, AX1 below Lake Wanaka and Lake Hawea, AX2 below Lake Wakatipu, AX4 and DN4 below AX1 and AX2, DN9 below Lake Te Anau and Lake Manapouri, and TK4 and TK6 below Lake Tekapo, Pukai, Ohau, Benmore, Aviemore and Waitaki. Elevated evaporation rates in the catchments above sites in these two areas could be partly responsible for differences in RWL slopes between the North and South Islands, and between NRWL and GMWL. Finally, lakes in the Rotorua and Taupo regions (such as Lake Tarawera, which feeds the Tarawera River, monitored by sites RO1 and RO2) are affected by geothermal activity which may increase the proportions of heavier stable isotopes in surface waters (Stewart et al., 1983). These results support previous research that indicates upstream lake area is a strong driver of river water isotope values at a global scale (Halder, Terzer, Wassenaar, Araguás-Araguás, & Aggarwal, 2015).

Spatial patterns of d-excess in river waters reflect variation of d-excess in precipitation sources, as well as processes of fractionation during evaporation from the surface waters themselves (West et al., 2014). Regions with highest long-term d-excess values of precipitation in New Zealand are in the north of the North Island, and windward sides of mountain ranges in both North and South Islands (Figure 8). Lowest values are in the south of the South Island, and in high-elevation leeward areas of mountain ranges across the country (Baisden et al., 2016). Patterns of d-excess values of river water shown in Figure 5 are largely reflective of precipitation patterns (Figure 8), with some exceptions; both the area around Lake Tarawera and Lake Rotoroa in the North Island, and in the Canterbury region of the South Island show d-excess values lower than might be expected based on d-excess in local precipitation. This result may be caused by increased evaporation due to upstream lake area and geothermal activity in the North Island Lakes area referred to above, and runoff from lakes, glaciers, and snow-cover in Canterbury. Notably, both these areas show high mean annual evaporative ratios (Figure 5d) and generally low humidity (Tait, 2008), which may lead to high expression of isotope effects in surface waters (Cappa, Hendricks, DePaolo, & Cohen, 2003). Particularly for the Canterbury Region, river water derived from high-elevation runoff is likely to show lower d-excess values than rainfall at low-elevations. The relatively low d-excess values in river water in Canterbury rivers may partly reflect the major source of their water being from precipitation at high elevations.

4.2 | Temporal patterns of river water $\delta^{18}O$ and $\delta^{2}H$ values

Across all sites, average seasonal offsets (amplitudes) for $\delta^{2}H$, and $\delta^{18}O$ (not shown) for NZRWQN sites were less than half of those of average values for rivers in the Global Network of Isotopes in Rivers (GNIR; Halder et al., 2015). This difference may be, firstly, due to the large catchment size represented by many of the NZRWQN sites; only 5 of the 58 sites in our current dataset drain catchments of less than 100 km^2. Large catchments tend to have greater catchment storage (e.g., as lakes and groundwater) causing damping of seasonal isotope variation in river waters (Halder et al., 2015; von Freyberg et al., 2018). This catchment storage may include water stored during winter as snow and ice, and subsequently released during spring and summer. The delay of minimum and maximum $\delta^{2}H$ in the South Island compared to the North Island may be due to greater snow and ice cover in winter, and lake storage in the South Island than in the North Island (Halder et al., 2015). Secondly, previously reported seasonal offsets of $\delta^{2}H$ and $\delta^{18}O$ in precipitation at GNIP stations in New Zealand are low for a country of New Zealand's latitude (Allen et al., 2019). Notably, the two operating GNIP stations in New Zealand are in the far north of the North Island and the south of the South Island, two areas of the country that have the lowest seasonal precipitation offsets based on the national-scale data of Baisden et al. (2016). The data of Baisden et al. (2016) and Marttila et al. (2017) support modelled values from Allen et al. (2019), which predict somewhat higher precipitation offset values within some central parts of the North and South Islands; Marttila et al. (2017), in inland Canterbury, found seasonal $\delta^{18}O$ offsets of $\sim$10‰ for precipitation, and $\sim$2.5–4‰ for stream water. Our findings support these general patterns; while seasonal offsets in river water were generally low, distinct seasonal patterns were observed across the country with the highest offsets observed in smaller catchments in central, inland South Island. Thus, inland mid-latitude areas of New Zealand would appear most appropriate for hydrological studies that examine timescales of storage in catchments using seasonal patterns of $\delta^{2}H$ and $\delta^{18}O$.

5 | CONCLUSION

In this paper, we studied the spatial distribution, seasonal variation, and environmental drivers of river water isotope values based on 2 years of monthly sampling from 58 sites selected to represent the spatial extent and varied geology, climate and other environmental aspects of New Zealand's river catchments. Below are our conclusions:

1. The distinctive difference in slope in the river water lines between the South Island and the North Island reflects different evaporation processes in these two islands, which are related to geographic characteristics (e.g., lake area) and climate characteristic (e.g., evaporative ratio). Spatial patterns of d-excess in precipitation also appear to contribute to the patterns observed, and further research is required to distinguish the relative influences of these processes;
2. The significant correlations between stable isotopes and environmental factors such as catchment slope and lake area suggest that spatial modelling of $\delta^{2}H$ and $\delta^{18}O$ with environmental factors across "dendritic" river networks (e.g., Bowen et al., 2011; Yang et al., 2017) would result in improved river water isotope predictions at finer scale, compared to method only based on distance

(i.e., IDW, nearest neighbour, and ordinary Kriging). This is the case because some factors observed to alter surface water isotope values (such as dams) will transfer their effects downstream but are no more likely to occur in neighbouring river networks than distant ones.

3. Although lower than those of rivers across the GNIR, average seasonal offsets for δ^2H, and $\delta^{18}O$ for NZRWQN sites show distinct seasonal patterns. Together with rainfall isotope data, these patterns could be used to in water age applications, such as derivation of young water fractions, across New Zealand. These applications may provide useful information to improve understanding of hydrologic process and aid surface- and groundwater quality management.

ACKNOWLEDGEMENT

This work is funded by New Zealand's Ministry for Business, Innovation and Employment via the NIWA Strategic Science Investment Fund (SSIF).

DATA AVAILABILITY STATEMENT

The data that support the findings will be available in the Global Network of Isotopes in Rivers (GNIR) of International Atomic Energy Agency (IAEA) through the WISER portal (Water Isotope System for Data Analysis, Visualization and Electronic Retrieval) following an embargo from the date of publication to allow for commercialization of research findings.

ORCID

Jing Yang https://orcid.org/0000-0002-6083-6286

REFERENCES

Ala-Aho, P., Soulsby, C., Pokrovsky, O. S., Kirpotin, S. N., Karlsson, J., Serikova, S., … Tetzlaff, D. (2018). Using stable isotopes to assess surface water source dynamics and hydrological connectivity in a high-latitude wetland and permafrost influenced landscape. *Journal of Hydrology*, *556*, 279–293.

Allen, S. T., Jasechko, S., Berghuijs, W. R., Welker, J. M., Goldsmith, G. R., & Kirchner, J. W. (2019). Global sinusoidal seasonality in precipitation isotopes. *Hydrology and Earth System Sciences*, *23*, 3423–3436.

Araguas-Araguas, L., & Diaz Teijeiro, M. (2005). Isotope composition of precipitation and water vapour in the Iberian Peninsula: First results of the Spanish network of isotopes in precipitation. *International Atomic Energy Agency Technical Report*, *1453*, 173–190.

Baisden, W. T., Keller, E. D., Van Hale, R., Frew, R. D., & Wassenaar, L. I. (2016). Precipitation isoscapes for New Zealand: Enhanced temporal detail using precipitation-weighted daily climatology. *Isotopes in Environmental and Health Studies*, *52*, 343–352.

Bowen, G. J. (2010). Isoscapes: Spatial pattern in isotopic biogeochemistry. *Annual Review of Earth and Planetary Sciences*, *38*, 161–187.

Bowen, G. J., Kennedy, C. D., Liu, Z., & Stalker, J. (2011). Water balance model for mean annual hydrogen and oxygen isotope distributions in surface waters of the contiguous United States. *Journal of Geophysical Research*, *116*(G4). http://dx.doi.org/10.1029/2010jg001581

Cable, J., Ogle, K., & Williams, D. (2011). Contribution of glacier meltwater to streamflow in the Wind River Range, Wyoming, inferred via a Bayesian mixing model applied to isotopic measurements. *Hydrological Processes*, *25*, 2228–2236.

Cappa, C. D., Hendricks, M. B., DePaolo, D. J., & Cohen, R. C. (2003). Isotopic fractionation of water during evaporation. *Journal of Geophysical Research: Atmospheres*, *108(D16)*(4525), 13-1–13-10.

Craig, H. (1961a). Isotopic variations in meteoric waters. *Science*, *133*, 1702–1703.

Craig, H. (1961b). Standard for reporting concentrations of deuterium and oxygen-18 in natural waters. *Science*, *133*, 1833–1834.

Dansgaard, W. (1954). The O^{18}-abundance in fresh water. *Geochimica et Cosmochimica Acta*, *6*, 241–260.

Dansgaard, W. (1964). Stable isotopes in precipitation. *Tellus*, *16*, 436–468.

Darling, W. G., Bath, A. H., & Talbot, J. C. (2003). The O and H stable isotope composition of freshwaters in the British Isles. 2, Surface waters and groundwater. *Hydrology and Earth System Sciences*, *7*, 183–195.

Davies-Colley, R. J., Smith, D. G., Ward, R. C., Bryers, G. G., McBride, G. B., Quinn, J. M., & Scarsbrook, M. R. (2011). Twenty years of New Zealand's National Rivers Water Quality Network: Benefits of careful design and consistent operation 1. *Journal of the American Water Resources Association*, *47*, 750–771.

Edwards, T. W., Wolfe, B. B., Gibson, J. J., & Hammarlund, D. (2004). Use of water isotope tracers in high latitude hydrology and paleohydrology. In *Long-term environmental change in Arctic and Antarctic lakes* (pp. 187–207). Dordrecht: Springer.

Feng, X., Faiia, A. M., & Posmentier, E. S. (2009). Seasonality of isotopes in precipitation: A global perspective. *Journal of Geophysical Research*, *114*(D8). http://dx.doi.org/10.1029/2008jd011279

Gammons, C. H., Poulson, S. R., Pellicori, D. A., Reed, P. J., Roesler, A. J., & Petrescu, E. M. (2006). The hydrogen and oxygen isotopic composition of precipitation, evaporated mine water, and river water in Montana, USA. *Journal of Hydrology*, *328*, 319–330.

Gao, Y., & Beamish, R. (1999). Isotopic composition of otoliths as a chemical tracer in population identification of sockeye salmon (*Oncorhynchus nerka*). *Canadian Journal of Fisheries and Aquatic Sciences*, *56*, 2062–2068.

Gibson, J. J., Birks, S. J., & Edwards, T. W. D. (2008). Global prediction of δ_A and δ^2H-$\delta^{18}O$ evaporation slopes for lakes and soil water accounting for seasonality. *Global Biogeochemical Cycles*, *22*(2). http://dx.doi.org/10.1029/2007gb002997

Gonfiantini, R., Fröhlich, K., Araguás-Araguás, L., & Rozanski, K. (1998). Chapter 7—Isotopes in groundwater hydrology. In C. Kendall & J. J. McDonnell (Eds.), *Isotope tracers in catchment hydrology* (pp. 203–246). Amsterdam: Elsevier.

Gonfiantini, R., Roche, M.-A., Olivry, J.-C., Fontes, J.-C., & Zuppi, G. M. (2001). The altitude effect on the isotopic composition of tropical rains. *Chemical Geology*, *181*, 147–167.

Halder, J., Terzer, S., Wassenaar, L., Araguás-Araguás, L., & Aggarwal, P. (2015). The Global Network of Isotopes in Rivers (GNIR): Integration of water isotopes in watershed observation and riverine research. *Hydrology and Earth System Sciences*, *19*, 3419–3431.

Hales, T., & Roering, J. (2009). A frost "buzzsaw" mechanism for erosion of the eastern Southern Alps, New Zealand. *Geomorphology*, *107*, 241–253.

IAEA/WMO, A. (2006). Global network of isotopes in precipitation. The GNIP database.

Isokangas, E., Rossi, P. M., Ronkanen, A.-K., Marttila, H., Rozanski, K., & Kløve, B. (2017). Quantifying spatial groundwater dependence in peatlands through a distributed isotope mass balance approach. *Water Resources Research*, *53*(3), 2524–2541. http://dx.doi.org/10.1002/2016wr019661

Jasechko, S., Kirchner, J. W., Welker, J. M., & McDonnell, J. J. (2016). Substantial proportion of global streamflow less than three months old. *Nature Geoscience*, *9*, 126–129.

Katsuyama, M., Yoshioka, T., & Konohira, E. (2015). Spatial distribution of oxygen-18 and deuterium in stream waters across the Japanese archipelago. *Hydrology and Earth System Sciences*, *19*, 1577–1588.

Kelly, S., Heaton, K., & Hoogewerff, J. (2005). Tracing the geographical origin of food: The application of multi-element and multi-isotope analysis. *Trends in Food Science & Technology*, *16*, 555–567.

Kendall, C., & Coplen, T. B. (2001). Distribution of oxygen-18 and deuterium in river waters across the United States. *Hydrological Processes*, *15*, 1363–1393.

Kirchner, J. W. (2016). Aggregation in environmental systems – Part 1: Seasonal tracer cycles quantify young water fractions, but not mean transit times, in spatially heterogeneous catchments. *Hydrology and Earth System Sciences*, *20*, 279–297.

Kirchner, J. W., & Allen, S. T. (2020). Seasonal partitioning of precipitation between streamflow and evapotranspiration, inferred from end-member splitting analysis. *Hydrology and Earth System Sciences*, *24*, 17–39.

Klaus, J., & McDonnell, J. (2013). Hydrograph separation using stable isotopes: Review and evaluation. *Journal of Hydrology*, *505*, 47–64.

Kortelainen, N. M., & Karhu, J. A. (2004). Regional and seasonal trends in the oxygen and hydrogen isotope ratios of Finnish groundwaters: A key for mean annual precipitation. *Journal of Hydrology*, *285*, 143–157.

Kuhlemann, L.-M., & Soulsby, C. (2020). Urban water systems under climate stress: An isotopic perspective from Berlin, Germany. *Hydrological Processes*, *34*, 3758–3776.

Lachniet, M. S., Moy, C. M., Riesselman, C. R., & Stephen, H. (2018). New Zealand river isoscapes document a stable isotopic rain shadow in the lee of the Southern Alps. AGUFM 2018:PP21F-1489.

Landwehr, J., & Coplen, T. (2006). Line-conditioned excess: A new method for characterizing stable hydrogen and oxygen isotope ratios in hydrologic systems. *Isotopes in Environmental Studies* (pp. 132–135). Monaco: International Atomic Energy Agency.

Leathwick, J. R., West, D., Chadderton, L., Gerbeaux, P., Kelly, D., & Robertson, H. (2010). *Freshwater Ecosystems of New Zealand (FENZ) Geodatabase: Version One – August 2010 – User Guide* (pp. 1–51). Department of Conservation: New Zealand.

Lutz, S. R., Krieg, R., Müller, C., Zink, M., Knöller, K., Samaniego, L., & Merz, R. (2018). Spatial patterns of water age: Using young water fractions to improve the characterization of transit times in contrasting catchments. *Water Resources Research*, *54*, 4767–4784.

Marttila, H., Dudley, B., Graham, S., & Srinivasan, M. (2017). Does transpiration from invasive stream side willows dominate low-flow conditions? An investigation using hydrometric and isotopic methods in a headwater catchment. *Ecohydrology*, *11*, e1930.

McDonnell, J. J., Stewart, M. K., & Owens, I. F. (1991). Effect of catchment-scale subsurface mixing on stream isotopic response. *Water Resources Research*, *27*, 3065–3073.

Négrel, P., Petelet-Giraud, E., Barbier, J., & Gautier, E. (2003). Surface water–groundwater interactions in an alluvial plain: Chemical and isotopic systematics. *Journal of Hydrology*, *277*, 248–267.

Putman, A. L., Fiorella, R. P., Bowen, G. J., & Cai, Z. (2019). A global perspective on local meteoric water lines: Meta-analytic insight into fundamental controls and practical constraints. *Water Resources Research*, *55*, 6896–6910.

R Core Team. (2018). *R: A language and environment for statistical computing*. Vienna, Austria: R Foundation for Statistical Computing.

Salinger, M., & Mullan, A. (1999). New Zealand climate: Temperature and precipitation variations and their links with atmospheric circulation 1930–1994. *International Journal of Climatology: A Journal of the Royal Meteorological Society*, *19*, 1049–1071.

Scholl, M. A., Ingebritsen, S. E., Janik, C. J., & Kauahikaua, J. P. (1996). Use of precipitation and groundwater isotopes to interpret regional hydrology on a tropical volcanic Island: Kilauea volcano area, Hawaii. *Water Resources Research*, *32*, 3525–3537.

Schotterer, U., Oldfield, F., & Fröhlich, K. (1996). GNIP. Global network for isotopes in precipitation.

Smith, D. G., & Maasdam, R. (1994). New Zealand's National River Water Quality Network 1. Design and physico-chemical characterisation. *New Zealand Journal of Marine and Freshwater Research*, *28*, 19–35.

Snelder, T. H., Biggs, B. J. F., & Woods, R. A. (2005). Improved eco-hydrological classification of rivers. *River Research and Applications*, *21*(6), 609–628. http://dx.doi.org/10.1002/rra.826

Soulsby, C., & Tetzlaff, D. (2008). Towards simple approaches for mean residence time estimation in ungauged basins using tracers and soil distributions. *Journal of Hydrology*, *363*, 60–74.

Sprenger, M., Tetzlaff, D., Tunaley, C., Dick, J., & Soulsby, C. (2017). Evaporation fractionation in a peatland drainage network affects stream water isotope composition. *Water Resources Research*, *53*, 851–866.

Starrs, D., Ebner, B. C., & Fulton, C. J. (2016). All in the ears: Unlocking the early life history biology and spatial ecology of fishes. *Biological Reviews*, *91*, 86–105.

Stewart, M. K., Cox, M. A., James, M. R., & Lyon, G. L. (1983). *Deuterium in New Zealand rivers and streams*. Lower Hutt: DSIR, Institute of Nuclear Sciences.

Stewart, M., & Taylor, C. (1981). Environmental isotopes in New Zealand hydrology. 1. Introduction: The role of oxygen-18. *New Zealand Journal of Science*, *24*, 295–311.

Tait, A. (2008). Future projections of growing degree days and frost in New Zealand and some implications for grape growing. *Weather and Climate*, *28*, 17–36.

Tait, A., Henderson, R., Turner, R., & Zheng, X. G. (2006). Thin plate smoothing spline interpolation of daily rainfall for New Zealand using a climatological rainfall surface. *International Journal of Climatology*, *26*, 2097–2115.

Taylor, C. B., Wilson, D. D., Brown, L. J., Stewart, M. K., Burden, R. J., & Brailsford, G. W. (1989). Sources and flow of north Canterbury plains groundwater, New Zealand. *Journal of Hydrology*, *106*, 311–340.

von Freyberg, J., Allen, S. T., Seeger, S., Weiler, M., & Kirchner, J. W. (2018). Sensitivity of young water fractions to hydro-climatic forcing and landscape properties across 22 Swiss catchments. *Hydrology and Earth System Sciences*, *22*, 3841–3861.

Wassenaar, L. I., Van Wilgenburg, S. L., Larson, K., & Hobson, K. A. (2009). A groundwater isoscape (δD, $\delta^{18}O$) for Mexico. *Journal of Geochemical Exploration*, *102*, 123–136.

West, A. G., February, E. C., & Bowen, G. J. (2014). Spatial analysis of hydrogen and oxygen stable isotopes ("isoscapes") in ground water and tap water across South Africa. *Journal of Geochemical Exploration*, *145*, 213–222.

Yang, J., McMillan, H., & Zammit, C. (2017). Modeling surface water–groundwater interaction in New Zealand: Model development and application. *Hydrological Processes*, *31*, 925–934.

How to cite this article: Yang J, Dudley BD, Montgomery K, Hodgetts W. Characterizing spatial and temporal variation in ^{18}O and ^{2}H content of New Zealand river water for better understanding of hydrologic processes. *Hydrological Processes*. 2020;1–15. https://doi.org/10.1002/hyp.13962